Quantum phase slip noise

Andrew G. Semenov[1,2] and Andrei D. Zaikin[1,3]
[1]*I. E. Tamm Department of Theoretical Physics, P. N. Lebedev Physical Institute, 119991 Moscow, Russia*
[2]*National Research University Higher School of Economics, 101000 Moscow, Russia*
[3]*Institute of Nanotechnology, Karlsruhe Institute of Technology (KIT), 76021 Karlsruhe, Germany*
(Received 8 March 2016; revised manuscript received 5 July 2016; published 18 July 2016)

Quantum phase slips (QPSs) generate voltage fluctuations in superconducting nanowires. Employing the Keldysh technique and making use of the phase-charge duality arguments, we develop a theory of QPS-induced voltage noise in such nanowires. We demonstrate that quantum tunneling of the magnetic flux quanta across the wire yields quantum shot noise which obeys Poisson statistics and is characterized by a power-law dependence of its spectrum S_Ω on the external bias. In long wires, S_Ω decreases with increasing frequency Ω and vanishes beyond a threshold value of Ω at $T \to 0$. The quantum coherent nature of QPS noise yields nonmonotonous dependence of S_Ω on T at small Ω.

DOI: 10.1103/PhysRevB.94.014512

I. INTRODUCTION

Can a superconductor generate voltage fluctuations? More specifically, if an external bias is applied to a superconductor, could the latter produce shot noise? By posing these questions, we, of course, imply that temperature T, characteristic frequencies and/or voltages, as well as all other relevant energy parameters remain well below the superconducting gap, i.e., the superconductor is either in or sufficiently close to its quantum ground state.

At first sight, positive answers to both of these questions can be rejected on fundamental grounds. Indeed, a superconducting state is characterized by zero resistance, i.e., a nondissipative current below some critical value can pass through the system. Hence, neither the nonzero average voltage nor voltage fluctuations can be expected.

These simple considerations—although applicable to bulk superconductors—become insufficient in the case of ultrathin superconducting wires because of the presence of quantum phase slips (QPSs) [1–4]. In such wires, quantum fluctuations of the superconducting order parameter field $\Delta = |\Delta|e^{i\varphi}$ play an important role, being responsible for temporal local suppression of $|\Delta|$ inside the wire and, hence, for the phase slippage process. Each quantum phase slip event corresponds to the net phase jump by $\delta\varphi = \pm 2\pi$, implying positive or negative voltage pulse $\delta V = \dot{\varphi}/2e$ (here and below, we set $\hbar = 1$) and tunneling of one magnetic flux quantum $\Phi_0 \equiv \pi/e = \int |\delta V(t)|dt$ across the wire in the direction perpendicular to its axis. Biasing the wire by an external current I, one breaks the symmetry between positive and negative voltage pulses, making the former more likely than the latter. As a result, the net voltage drop V occurs across the wire, also implying nonzero resistance $R = V/I$ which may not vanish down to lowest T [5,6], as it was indeed observed in a number of experiments [7–9]. Hence, in the presence of QPSs, the current flow becomes dissipative and—according, e.g., to the fluctuation-dissipation theorem (FDT)—one should also expect voltage fluctuations to occur in the system.

While these arguments suggest a positive answer to the first of the above questions, they do not yet specifically address shot noise. Two key prerequisites of shot noise are (i) the presence of discrete charge carriers (e.g., electrons) in the system and (ii) scattering of such carriers at disorder. Although discrete charge carriers—Cooper pairs—are certainly present in superconducting nanowires, they form a superconducting condensate flowing along the wire *without any scattering*. For this reason, the possibility for shot noise to occur in superconducting nanowires appears by no means obvious.

In this paper, we will perform a detailed theoretical analysis of QPS-induced voltage fluctuations in ultrathin superconducting wires. In particular, we will demonstrate that quantum tunneling of magnetic flux quanta Φ_0 across the wire causes shot noise which obeys Poisson statistics and shows a nontrivial dependence on temperature, frequency, and external current.

II. THE MODEL AND EFFECTIVE HAMILTONIAN

The system under consideration is displayed in Fig. 1. It consists of an ultrathin superconducting wire of length L and cross section s, and a capacitance C switched in parallel to this wire. The right end of the wire ($x = L$) is grounded, as shown in the figure (x is the coordinate along the wire ranging from 0 to L). The voltage $V(t)$ at its left end $x = 0$ fluctuates and such fluctuations can be measured by a detector. The whole system is biased by an external current $I = V_x/R_x$.

An effective Hamiltonian for our system can be written in the form

$$\hat{H} = \hat{H}_{\rm Ch} - I\varphi/2e + \hat{H}_{\rm wire}. \tag{1}$$

The first and the second terms in the right-hand side of Eq. (1) account, respectively, for the charging energy [10],

$$\hat{H}_{\rm Ch} = \frac{1}{2C}\left[-i\frac{\partial}{\partial(\varphi/2e)} + Q\right]^2, \tag{2}$$

and for the potential energy tilt produced by an external current I. The variable $\varphi(t) \equiv \varphi(0,t)$ represents the phase of the superconducting order parameter field $\Delta(x,t)$ at $x = 0$. Here we also set $\varphi(L,t) \equiv 0$.

The last term $\hat{H}_{\rm wire}$ in Eq. (1) describes the superconducting wire. This part of the effective Hamiltonian can be expressed in terms of both the modulus $|\Delta(x,t)|$ and the phase $\varphi(x,t)$ of the order parameter field [5,6,11]. Here, however, we will proceed differently and employ the duality arguments.

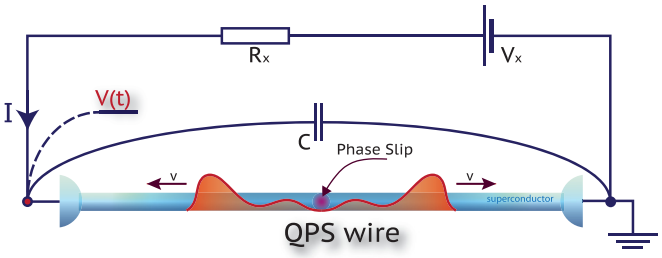

FIG. 1. The system under consideration. The figure also illustrates creation of two plasmons by a QPS.

The duality between the phase and the charge variables was established and discussed in detail in the case of ultrasmall Josephson junctions [10,12–14]. Later the same duality arguments were extended to short [15] and long [16–18] superconducting wires. According to the results [18], the dual representation for the Hamiltonian of a superconducting nanowire is defined by an effective sine-Gordon model,

$$\hat{H}_{\rm wire} = \hat{H}_{\rm TL} + \hat{H}_{\rm QPS}. \tag{3}$$

In the absence of quantum phase slips, such nanowire can be described as a transmission line with

$$\hat{H}_{\rm TL} = \int_0^L dx \left[\frac{\Phi^2}{2\mathcal{L}_{\rm kin}} + \frac{(\partial_x \chi)^2}{2C_{\rm w}\Phi_0^2} \right], \tag{4}$$

where $\mathcal{L}_{\rm kin} = 1/(\pi\sigma_N \Delta_0 s)$ and $C_{\rm w}$ are, respectively, the kinetic wire inductance (times length) and the geometric wire capacitance (per length),

$$[\Phi(x), \chi(x')] = -i\Phi_0 \delta(x - x') \tag{5}$$

defines the commutation relation between the canonically conjugate flux (or phase) and charge operators, σ_N is the normal-state Drude conductance of the wire, and Δ_0 is the superconducting gap. The term

$$\hat{H}_{\rm QPS} = -\gamma_{\rm QPS} \int_0^L dx \cos\chi \tag{6}$$

accounts for the effect of quantum phase slips and

$$\gamma_{\rm QPS} \sim (g_\xi \Delta_0/\xi) \exp(-a g_\xi), \quad a \sim 1, \tag{7}$$

is the QPS tunneling amplitude [6] per unit wire length, with $g_\xi = 2\pi\sigma_N s/(e^2\xi) \gg 1$ being the dimensionless normal-state conductance of the wire segment of length equal to the coherence length ξ.

The physical meaning of the quantum field $\chi(x,t)$ is transparent: It is proportional to the total charge $q(x,t)$ that has passed through the point x up to the time moment t, i.e., $q(x,t) = \chi(x,t)/\Phi_0$. Accordingly, the local current $I(x,t)$ and the local charge density $\rho(x,t)$ are defined as

$$I(x,t) = \partial_t \chi(x,t)/\Phi_0, \quad \rho(x,t) = -\partial_x \chi(x,t)/\Phi_0, \tag{8}$$

thereby satisfying the continuity equation. The charge Q in Eq. (2) is equal to $Q(t) = \chi(0,t)/\Phi_0$.

III. KELDYSH TECHNIQUE AND PERTURBATION THEORY

In order to proceed, we will make use of the Keldysh path-integral technique. Accordingly, our variables of interest need to be defined on the forward and backward time branches of the Keldysh contour, i.e., we now have $\varphi_{F,B}(t)$ and $\chi_{F,B}(x,t)$. As usual, it is convenient to also introduce the "classical" and "quantum" variables, respectively, $\varphi_+(t) = [\varphi_F(t) + \varphi_B(t)]/2$ and $\varphi_-(t) = \varphi_F(t) - \varphi_B(t)$ (and similarly for the χ fields). Making use of the Josephson relation between the voltage and the phase, one can formally express the expectation value of the voltage operator across the superconducting wire in the form

$$\langle V(t_1)\rangle = \frac{1}{2e}\langle \dot{\varphi}_+(t_1) e^{iS_{\rm QPS}}\rangle_0, \tag{9}$$

where

$$S_{\rm QPS} = -2\gamma_{\rm QPS} \int dt \int_0^L dx \sin(\chi_+)\sin(\chi_-/2), \tag{10}$$

and

$$\langle \ldots \rangle_0 = \int \mathcal{D}^2\varphi(t)\mathcal{D}^2\chi(x,t)(\ldots)e^{iS_0[\varphi,\chi]} \tag{11}$$

implies averaging with the Keldysh effective action S_0 corresponding to the Hamiltonian $\hat{H}_0 = \hat{H} - \hat{H}_{\rm QPS}$. Analogously, for the voltage-voltage correlator $\langle V(t_1)V(t_2)\rangle = \frac{1}{2}\langle\{\hat{V}(t_1), \hat{V}(t_2)\}\rangle$ (where curly brackets denote the anticommutator), one has

$$\langle V(t_1)V(t_2)\rangle = \frac{1}{4e^2}\langle \dot{\varphi}_+(t_1)\dot{\varphi}_+(t_2) e^{iS_{\rm QPS}}\rangle_0. \tag{12}$$

Higher-voltage correlators are defined similarly. Their analysis, however, is beyond the scope of this work.

Equations (9) and (12) are formally exact expressions, which we are now going to evaluate. To this end, we will employ the regular perturbation theory in $\gamma_{\rm QPS}$ (7), which can be regarded as a small parameter of our theory. In the zero order in $\gamma_{\rm QPS}$, the problem is described by the quadratic (in both φ and χ) Hamiltonian $\hat{H}_0$ and all averages can be handled exactly with the aid of the Green functions,

$$\begin{aligned} G^R_{ab}(X,X') &= -i\langle a_+(X) b_-(X')\rangle, \\ G^K_{ab}(X,X') &= -i\langle a_+(X) b_+(X')\rangle, \end{aligned} \tag{13}$$

where $a(X)$ and $b(X)$ stand for one of the fields $\varphi(t)$ and $\chi(x,t)$. As both of these fields are real, the advanced and retarded Green functions obey the condition $G^A_{ab}(\omega) = G^R_{ba}(-\omega)$. With this in mind, the Keldysh function G^K can be expressed in the form

$$G^K_{ab}(\omega) = \frac{1}{2}\coth\left(\frac{\omega}{2T}\right)\left[G^R_{ab}(\omega) - G^R_{ba}(-\omega)\right]. \tag{14}$$

Expanding Eqs. (9) and (12) up to the second order in $\gamma_{\rm QPS}$ and performing all necessary averages, we evaluate the results in terms of the Green functions (13); see the Appendices for further details. The result of our calculation both for the average voltage (9) and for the voltage-voltage correlator (12) can also be expressed in the form of "candy" diagrams, displayed in Fig. 2. They involve four different propagators

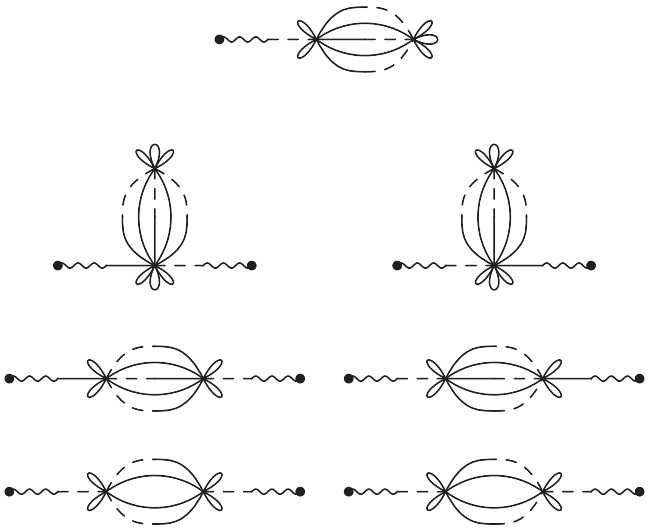

FIG. 2. Candylike diagrams which determine both average voltage (9) (upper diagram) and voltage noise (12) (six remaining diagrams) in the second order in $\gamma_{\rm QPS}$. The fields φ_+, χ_+, and χ_- in the propagators (13) are denoted, respectively by wavy, solid, and dashed lines.

($G^{R,K}_{\chi\chi}$ and $G^{R,K}_{\varphi\chi}$) and plenty of vertices originating from Taylor expansion of the cosine terms. Summing up all of the diagrams in the same order in $\gamma_{\rm QPS}$, one arrives at the final expression containing the exponents of the Green functions.

IV. $I-V$ CURVE AND VOLTAGE NOISE

To begin with, let us briefly rederive the results [5] for the average voltage within the framework of our technique. We obtain (see Appendix A)

$$\langle V\rangle = \frac{i\gamma_{\rm QPS}^2}{4e}\int_0^L dx\int_0^L dx'\Big[\lim_{\omega\to 0}\omega G^R_{\varphi\chi}(x;\omega)\Big] \times[\mathcal{P}_{x,x'}(-\Phi_0 I)-\mathcal{P}_{x,x'}(\Phi_0 I)], \tag{15}$$

where $\mathcal{P}_{x,x'}(\omega)=P_{x,x'}(\omega)+\bar{P}_{x,x'}(\omega)$ and

$$P_{x,x'}(\omega)=\int_0^\infty dt e^{i\omega t}e^{i\mathcal{G}(x,x';t,0)}, \tag{16}$$

$$\mathcal{G}(x,x';t,0)=G^K_{\chi\chi}(x,x';t,0)-\frac{1}{2}G^K_{\chi\chi}(x,x;t,t) -\frac{1}{2}G^K_{\chi\chi}(x',x';0,0)+\frac{1}{2}G^R_{\chi\chi}(x,x';t,0).$$

Bearing in mind that $\lim_{\omega\to 0}\omega G^R_{\varphi\chi}(x;\omega)=2\pi i$, Eq. (15) can be cast in the form

$$\langle V\rangle=\Phi_0[\Gamma_{\rm QPS}(I)-\Gamma_{\rm QPS}(-I)], \tag{17}$$

where we identify $\Gamma_{\rm QPS}$ as

$$\Gamma_{\rm QPS}(I)=\frac{\gamma_{\rm QPS}^2}{2}\int_0^L dx\int_0^L dx'\mathcal{P}_{x,x'}(\Phi_0 I). \tag{18}$$

Comparing the result (17) with that found in Ref. [5], we immediately conclude that $\Gamma_{\rm QPS}(I)$ defines the quantum decay rate of the current state due to QPS. In [5], this rate was evaluated from the imaginary part of the free energy, $\Gamma_{\rm QPS}(I)=2{\rm Im}F$. Here we derived the expression for $\Gamma_{\rm QPS}$ by means of the real-time technique without employing the ImF method.

Making use of the above results, evaluating the Green functions (13) (see Appendix C), and keeping in mind the detailed balance condition (see Appendix B),

$$\mathcal{P}_{x,x'}(\omega)=e^{\frac{\omega}{T}}\mathcal{P}_{x,x'}(-\omega), \tag{19}$$

we obtain

$$\langle V\rangle=\frac{\Phi_0 L v\gamma_{\rm QPS}^2}{2}\varsigma^2\left(\frac{\Phi_0 I}{2}\right)\sinh\left(\frac{\Phi_0 I}{2T}\right), \tag{20}$$

where $v=1/\sqrt{\mathcal{L}_{\rm kin}C_{\rm w}}$ is the plasmon velocity [19],

$$\varsigma(\omega)=\tau_0^\lambda(2\pi T)^{\lambda-1}\frac{\Gamma\left(\frac{\lambda}{2}-\frac{i\omega}{2\pi T}\right)\Gamma\left(\frac{\lambda}{2}+\frac{i\omega}{2\pi T}\right)}{\Gamma(\lambda)}, \tag{21}$$

$\tau_0\sim 1/\Delta_0$ is the QPS core size in time, and $\Gamma(x)$ is the Gamma function. Here we also introduced the parameter [5] $\lambda=R_q/2Z_{\rm w}\propto\sqrt{s}$, where $R_q=\pi/2e^2$ is the "superconducting" quantum resistance unit and $Z_{\rm w}=\sqrt{\mathcal{L}_{\rm kin}/C_{\rm w}}$ is the wire impedance. It is satisfactory to observe that the results (20) and (21) match that found in Ref. [5] by means of a different technique [20].

Let us now turn to voltage fluctuations. Our perturbative analysis, which we describe in Appendix A, allows one to recover three different contributions to the noise power spectrum, i.e.,

$$S_\Omega=\int dt e^{i\Omega t}\langle V(t)V(0)\rangle=S^{(0)}_\Omega+S^r_\Omega+S^a_\Omega. \tag{22}$$

The first of these contributions $S^{(0)}_\Omega$ has nothing to do with QPS and just defines equilibrium voltage noise for a transmission line. It reads

$$S^{(0)}_\Omega=\frac{i\Omega^2\coth\left(\frac{\Omega}{2T}\right)}{16e^2}\big[G^R_{\varphi\varphi}(\Omega)-G^R_{\varphi\varphi}(-\Omega)\big]. \tag{23}$$

The other two terms are due to QPS effects. The term S^r_Ω is also proportional to $\coth\left(\frac{\Omega}{2T}\right)$ and contains the products of two retarded (advanced) Green functions:

$$S^r_\Omega=\frac{\gamma_{\rm QPS}^2\Omega^2\coth\left(\frac{\Omega}{2T}\right)}{8e^2}\int_0^L dx\int_0^L dx'{\rm Re}\big\{G^R_{\varphi\chi}(x;\Omega) \times\big[\mathcal{F}_{x,x'}(\Omega)G^R_{\varphi\chi}(x';\Omega)-\mathcal{F}_{x,x'}(0)G^R_{\varphi\chi}(x;\Omega)\big]\big\}. \tag{24}$$

Here we denote

$$\mathcal{F}_{x,x'}(\Omega)=-P_{x,x'}(\Omega+\Phi_0 I)-P_{x,x'}(\Omega-\Phi_0 I) +\bar{P}_{x,x'}(-\Omega+\Phi_0 I)+\bar{P}_{x,x'}(-\Omega-\Phi_0 I). \tag{25}$$

The remaining term S^a_Ω, in contrast, contains the product of one retarded and one advanced Green function and scales with the combinations $\mathcal{C}_\pm=\coth\left(\frac{\Omega\pm\Phi_0 I}{2T}\right)-\coth\left(\frac{\Omega}{2T}\right)$ as

$$S^a_\Omega=\frac{\gamma_{\rm QPS}^2\Omega^2}{16e^2}\int_0^L dx\int_0^L dx' G^R_{\varphi\chi}(x;\Omega)G^R_{\varphi\chi}(x';-\Omega) \times\left\{\sum_\pm\mathcal{C}_\pm\big[\mathcal{P}_{x,x'}(\Omega\pm\Phi_0 I)-\mathcal{P}_{x,x'}(-\Omega\mp\Phi_0 I)\big]\right\}. \tag{26}$$

Equations (22)–(26) together with the expressions for the Green functions [Eqs. (C1)–(C3)] fully determine the voltage noise power spectrum of a superconducting nanowire in the perturbative in QPS regime and represent the central result of this work.

In the zero-bias limit $I \to 0$, the term S^a_Ω vanishes, and the equilibrium noise spectrum $S_\Omega = S^{(0)}_\Omega + S^r_\Omega$ is determined from FDT; see also [18]. At nonzero-bias values, the QPS noise turns nonequilibrium. In the zero-frequency limit $\Omega \to 0$, the terms $S^{(0)}_\Omega$ and S^r_Ω tend to zero, and the voltage noise $S_{\Omega\to 0} \equiv S_0$ is determined solely by S^a_Ω. Then, from Eq. (26), we obtain

$$S_0 = \Phi_0^2[\Gamma_{\rm QPS}(I) + \Gamma_{\rm QPS}(-I)] = \Phi_0 \coth\left(\frac{\Phi_0 I}{2T}\right)\langle V\rangle, \quad (27)$$

where $\langle V\rangle$ is specified in Eqs. (17) and (20). Combining the result (27) with Eqs. (20) and (21), we find

$$S_0 \propto \begin{cases} T^{2\lambda-2}, & T \gg \Phi_0 I, \\ I^{2\lambda-2}, & T \ll \Phi_0 I. \end{cases} \quad (28)$$

At higher temperatures $T \gg \Phi_0 I$ (though still $T \ll \Delta_0$), Eq. (28) just describes equilibrium voltage noise $S_0 = 2TR$ of a linear ohmic resistor $R = \langle V\rangle/I \propto T^{2\lambda-3}$ [5]. In the opposite low-temperature limit $T \ll \Phi_0 I$, it accounts for QPS-induced *shot noise* $S_0 = \Phi_0\langle V\rangle$ obeying *Poisson statistics* with an effective "charge" equal to the flux quantum Φ_0.

This result sheds light on the physical origin of shot noise in superconducting nanowires: It is produced by coherent tunneling of magnetic flux quanta Φ_0 across the wire. In the dual picture [18], such flux quanta can be viewed as charged quantum particles passing through (and being scattered at) an effective spatially extended tunnel barrier.

Note that previously the result analogous to Eq. (27) was derived for thermally activated phase slips (TAPSs) [21]. This similarity appears remarkable given a crucial physical difference between TAPSs and QPSs: The former can be regarded as classical (i.e., incoherent) and noninteracting objects, whereas the latter are fully coherent [22], forming an interacting quantum gas.

Another interesting limiting case is that of sufficiently high frequencies and/or long wires, $v/L \ll \Omega \ll \Delta_0$. In this limit, we obtain

$$S^{(0)}_\Omega = \frac{\lambda}{8\pi e^2}\frac{\Omega\coth\left(\frac{\Omega}{2T}\right)}{(\Omega/2E_C)^2 + (\lambda/\pi)^2}. \quad (29)$$

This contribution is independent of the wire length L. At low T and $\Omega/\lambda \gtrsim E_C = e^2/2C$, we have $S^{(0)}_\Omega \propto 1/\Omega$, i.e., the wire may generate $1/f$ voltage noise. Evaluating the QPS terms S^r_Ω and S^a_Ω, we observe that the latter scales linearly with the wire length L, whereas the former does not. Hence, the term S^r_Ω can be safely neglected in the long-wire limit. For the remaining QPS term S^a_Ω, we get

$$S^a_\Omega = \frac{L\lambda^2 v\gamma^2_{\rm QPS}}{4e^2}\left[\varsigma\left(\frac{\Phi_0 I}{2} - \Omega\right) - \varsigma\left(\frac{\Phi_0 I}{2} + \Omega\right)\right] \times \frac{\sinh\left(\frac{\Phi_0 I}{2T}\right)\varsigma\left(\frac{\Phi_0 I}{2}\right)}{\left[(\Omega/2E_C)^2 + (\lambda/\pi)^2\right]\sinh\left(\frac{\Omega}{2T}\right)}. \quad (30)$$

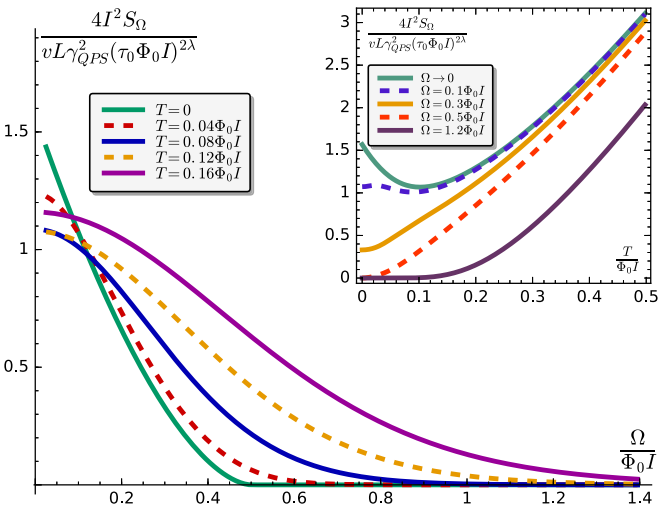

FIG. 3. The frequency dependence of the QPS noise spectrum S_Ω (30) at $\lambda = 2.7$, large E_C, and different T in the long-wire limit. The inset shows S_Ω as a function of T.

At $T \to 0$, from Eq. (30), we find

$$S^a_\Omega \propto \begin{cases} I^{\lambda-1}(I - 2\Omega/\Phi_0)^{\lambda-1}, & \Omega < \Phi_0 I/2 \\ 0, & \Omega > \Phi_0 I/2. \end{cases} \quad (31)$$

This result can be interpreted as follows. At $T = 0$, each QPS event excites (at least) two plasmons [23] (see Fig. 1) with total envergy $E = \Phi_0 I$ propagating in the opposite directions along the wire. One plasmon (with energy $E/2$) gets dissipated at the grounded end of the wire, while another one (also with energy $E/2$) reaches its opposite end causing voltage fluctuations (emits a photon) with frequency Ω measured by a detector. Clearly, at $T = 0$, this process is only possible at $\Omega < E/2$, in agreement with Eq. (31).

The result (30) is also illustrated in Fig. 3. At sufficiently small Ω (we still keep $\Omega \gg v/L$), one observes a nonmonotonous dependence of S_Ω on T, which is a direct consequence of the quantum coherent nature of QPS noise.

Finally, we point out that the perturbative in $\gamma_{\rm QPS}$ approach employed here is fully justified for not-too-thin wires with $\lambda > \lambda_c \simeq 2$ [5]. In wires with $\lambda < \lambda_c$ (characterized by unbound QPS–anti-QPS pairs), $\gamma_{\rm QPS}$ gets effectively renormalized to higher values and, hence, the perturbation theory eventually becomes obsolete. However, even in this case, our results may still remain applicable at sufficiently high temperature, frequency, and/or current values. In the low-energy limit, long wires with $\lambda < \lambda_c$ show an insulating behavior, as follows from the exact solution of the corresponding sine-Gordon model [24]. This solution suggests that voltage fluctuations also become large in this limit.

In summary, we demonstrated that quantum phase slips generate voltage noise in superconducting nanowires. In the presence of a current bias I, quantum tunneling of the magnetic flux quanta Φ_0 across the wire causes Poissonian shot noise

with a nontrivial power-law dependence of its spectrum on both I and frequency Ω. Our predictions can be directly verified in future experiments and need to be observed while optimizing the operation of QPS qubits [25].

ACKNOWLEDGMENTS

We acknowledge useful discussions with K. Yu. Arutyunov, D. S. Golubev, and P. Hakonen. This work was supported in part by RFBR Grant No. 15-02-08273.

APPENDIX A: PERTURBATION THEORY

Let us expand the general expressions (9) and (12) up to the second order in $\gamma_{\rm QPS}$. It is easy to demonstrate that linear in $\gamma_{\rm QPS}$ terms vanish identically in both expressions after averaging over the zero mode contained in the χ field. In order to evaluate the terms $\sim\gamma_{\rm QPS}^2$, it is convenient to make a shift $\chi_+(t)\to\Phi_0 It+\chi_+(t)$ and to decompose the averages by means of the Wick theorem. As a result, we obtain

$$\langle V(t_1)\rangle = -\frac{\gamma_{\rm QPS}^2}{e}\int dt\int_0^L dx\int dt'\int_0^L dx'\langle\dot\varphi_+(t_1)\chi_-(x,t)\rangle_0\langle\cos[\Phi_0 I(t-t')+\chi_+(x,t)-\chi_+(x',t')] \times\cos[\chi_-(x,t)/2]\sin[\chi_-(x',t')/2]\rangle_0, \tag{A1}$$

and

$$\begin{aligned}\langle V(t_1)V(t_2)\rangle = {}& \frac{1}{4e^2}\langle\dot\varphi_+(t_1)\dot\varphi_+(t_2)\rangle_0 - \frac{\gamma_{\rm QPS}^2}{2e^2}\int dt\int_0^L dx\int dt'\int_0^L dx'\langle\dot\varphi_+(t_1)\chi_+(x,t)\rangle_0\langle\dot\varphi_+(t_2)\chi_-(x,t)\rangle_0\\ &\times\langle\sin[\Phi_0 I(t'-t)+\chi_+(x',t')-\chi_+(x,t)]\cos[\chi_-(x,t)/2]\sin[\chi_-(x',t')/2]\rangle_0\\ &-\frac{\gamma_{\rm QPS}^2}{2e^2}\int dt\int_0^L dx\int dt'\int_0^L dx'\langle\dot\varphi_+(t_1)\chi_+(x,t)\rangle_0\langle\dot\varphi_+(t_2)\chi_-(x',t')\rangle_0\\ &\times\langle\sin[\Phi_0 I(t'-t)+\chi_+(x',t')-\chi_+(x,t)]\sin[\chi_-(x,t)/2]\cos[\chi_-(x',t')/2]\rangle_0\\ &-\frac{\gamma_{\rm QPS}^2}{2e^2}\int dt\int_0^L dx\int dt'\int_0^L dx'\langle\dot\varphi_+(t_1)\chi_-(x,t)\rangle_0\langle\dot\varphi_+(t_2)\chi_+(x,t)\rangle_0\\ &\times\langle\sin[\Phi_0 I(t'-t)+\chi_+(x',t')-\chi_+(x,t)]\cos[\chi_-(x,t)/2]\sin[\chi_-(x',t')/2]\rangle_0\\ &-\frac{\gamma_{\rm QPS}^2}{2e^2}\int dt\int_0^L dx\int dt'\int_0^L dx'\langle\dot\varphi_+(t_1)\chi_-(x,t)\rangle_0\langle\dot\varphi_+(t_2)\chi_+(x',t')\rangle_0\\ &\times\langle\sin[\Phi_0 I(t-t')+\chi_+(x,t)-\chi_+(x',t')]\cos[\chi_-(x,t)/2]\sin[\chi_-(x',t')/2]\rangle_0\\ &-\frac{\gamma_{\rm QPS}^2}{4e^2}\int dt\int_0^L dx\int dt'\int_0^L dx'\langle\dot\varphi_+(t_1)\chi_-(x,t)\rangle_0\langle\dot\varphi_+(t_2)\chi_-(x',t')\rangle_0\\ &\times\langle\cos[\Phi_0 I(t-t')+\chi_+(x,t)-\chi_+(x',t')]\cos[\chi_-(x,t)/2]\cos[\chi_-(x',t')/2]\rangle_0.\end{aligned} \tag{A2}$$

The averages in Eqs. (A1) and (A2) are Gaussian and, hence, can be handled in a straightforward manner. After that, we immediately arrive at our final results for the $I-V$ curve (15), (16) and for the voltage noise spectrum (22)–(26). Both of these results are expressed via the function $P_{x,x'}(\omega)$ (16), which in turn contains the Green function $\mathcal{G}(x,x';t,0)$.

APPENDIX B: ANALYTIC STRUCTURE OF THE GREEN FUNCTIONS

Let us define a more general Green function $\mathcal{G}_\chi(x,x';\sigma)$, which depends on the complex time σ and obeys the condition $\mathcal{G}_\chi(x,x';t-i0)=\mathcal{G}(x,x';t,0)$. With the aid of the Kubo-Martin-Schwinger condition, one can deduce that the Green function $\mathcal{G}_\chi$ is periodic in the imaginary-time direction, i.e.,

$$\mathcal{G}_\chi(x,x';\sigma)=\mathcal{G}_\chi(x,x';\sigma-i/T). \tag{B1}$$

This function is analytic and has branch cuts at $\mathrm{Im}(\sigma)=N/T$ for all integers N. The function $\exp[i\mathcal{G}_\chi(x,x';\sigma)]$ has the same analytic properties. One can write

$$\mathcal{P}_{x,x'}(\omega)=\int_{-\infty}^{\infty}dt e^{i\omega t}e^{i\mathcal{G}_\chi(x,x';t-i0)}. \tag{B2}$$

Distorting the integration path and utilizing the property $\mathcal{G}_\chi(x,x';\sigma)=-\bar{\mathcal{G}}_\chi(x,x';-\sigma)$ together with Eq. (B1), we arrive at the detailed balance condition (19).

APPENDIX C: GREEN FUNCTIONS

The Green functions for the system displayed in Fig. 1 can be evaluated directly with the following results:

$$G^R_{\varphi\varphi}(\omega) = \frac{1}{\frac{\omega^2}{2E_C} + \frac{i\omega}{4e^2R_x} - \frac{\omega\lambda}{\pi}\cot\left(\frac{\omega L}{v}\right)}, \tag{C1}$$

$$G^R_{\chi\varphi}(x;\omega) = -G^R_{\varphi\chi}(x;\omega) = \frac{2i\lambda\cos\left[\frac{\omega(L-x)}{v}\right]}{\left(\frac{\omega^2}{2E_C} + \frac{i\omega}{4e^2R_x}\right)\sin\left(\frac{\omega L}{v}\right) - \frac{\omega\lambda}{\pi}\cos\left(\frac{\omega L}{v}\right)}, \tag{C2}$$

and

$$G^R_{\chi\chi}(x,x';\omega) = \frac{4\pi\lambda\left\{\cos\left[\frac{\omega(L-x)}{v}\right]\cos\left(\frac{\omega x'}{v}\right)\theta(x-x') + \cos\left[\frac{\omega(L-x')}{v}\right]\cos\left(\frac{\omega x}{v}\right)\theta(x'-x)\right\}}{\omega\sin\left(\frac{\omega L}{v}\right)} + \frac{4\lambda^2\cos\left[\frac{\omega(L-x)}{v}\right]\cos\left[\frac{\omega(L-x')}{v}\right]}{\sin\left(\frac{\omega L}{v}\right)\left[\left(\frac{\omega^2}{2E_C} + \frac{i\omega}{4e^2R_x}\right)\sin\left(\frac{\omega L}{v}\right) - \frac{\omega\lambda}{\pi}\cos\left(\frac{\omega L}{v}\right)\right]}. \tag{C3}$$

The last two expressions take a much simpler form in the long-wire limit, in which case all plasmon excitations moving towards the grounded end of the wire eventually disappear and never pop up again, while excitations moving in the opposite direction produce voltage fluctuations measured by a detector. In this limit, Eqs. (C1) and (C3) reduce to

$$G^R_{\varphi\chi}(x;\omega) \simeq -\frac{2\lambda e^{i\frac{\omega x}{v}}}{(\omega+i0)\left(\frac{\omega}{2E_C} + \frac{i\lambda}{\pi}\right)}, \tag{C4}$$

$$G^R_{\chi\chi}(x,x';\omega) \simeq -\frac{2\pi i\lambda}{\omega+i0}e^{i\frac{\omega|x-x'|}{v}}. \tag{C5}$$

Here we also set $R_x \to \infty$, as requested in the current bias limit.

In order to evaluate the general expressions for the $I-V$ curve (15), (16) and for the voltage noise (22)–(26), it is necessary to compute the integral

$$\Upsilon(\omega,\Omega) = \int_{-L/2}^{L/2} dx \int_{-L/2}^{L/2} dx' e^{i\frac{\Omega}{v}(x-x')}\mathcal{P}_{x,x'}(\omega). \tag{C6}$$

Separating the left movers and the right movers, making use of the explicit form of the Green function $G^R_{\chi\chi}(x,x';\omega)$, and introducing the high-frequency cutoff $\omega_c \sim 1/\tau_0$ in order to avoid unphysical divergencies, we obtain

$$\Upsilon(\omega,\Omega) \simeq L\int_{-\infty}^{\infty} dx e^{i\frac{\Omega}{v}x}\mathcal{P}_{x,0}(\omega) = \frac{Lv}{2}\varpi\left(\frac{\omega}{2}+\frac{\Omega}{2}\right)\varpi\left(\frac{\omega}{2}-\frac{\Omega}{2}\right), \tag{C7}$$

where

$$\varpi(z) = \int_{-\infty}^{\infty} dt e^{izt}\frac{\sinh^{\lambda}(\pi T\tau_0)}{\sinh^{\lambda/2}[\pi T(\tau_0 - t + i0)]\sinh^{\lambda/2}[\pi T(\tau_0 + t - i0)]}. \tag{C8}$$

Performing the integration in Eq. (C8), we find

$$\varpi(\omega) = \frac{2^{\lambda}(\pi T\tau_0)^{\lambda}}{2\pi T}\frac{\Gamma\left(\frac{\lambda}{2} - \frac{i\omega}{2\pi T}\right)\Gamma\left(\frac{\lambda}{2} + \frac{i\omega}{2\pi T}\right)e^{\frac{\omega}{2T}}}{\Gamma(\lambda)} \equiv \varsigma(\omega)e^{\frac{\omega}{2T}}. \tag{C9}$$

The function $\varsigma(\omega)$ (21) is directly employed in our results, both for the $I-V$ curve (20) and for the QPS noise spectrum (27), (30).

[1] K. Yu. Arutyunov, D. S. Golubev, and A. D. Zaikin, Phys. Rep. **464**, 1 (2008).

[2] A. Bezryadin, J. Phys.: Condens. Matter **20**, 043202 (2008).

[3] A. D. Zaikin, in *Handbook of Nanophysics: Nanotubes and Nanowires* (CRC, Boca Raton, FL, 2010), p. 40-1.

[4] A. Bezryadin, *Superconductivity in Nanowires* (Wiley-VCH, Weinheim, 2013).

[5] A. D. Zaikin, D. S. Golubev, A. van Otterlo, and G. T. Zimányi, Phys. Rev. Lett. **78**, 1552 (1997).

[6] D. S. Golubev and A. D. Zaikin, Phys. Rev. B **64**, 014504 (2001).

[7] A. Bezryadin, C. N. Lau, and M. Tinkham, Nature (London) **404**, 971 (2000).

[8] C. N. Lau, N. Markovic, M. Bockrath, A. Bezryadin, and M. Tinkham, Phys. Rev. Lett. **87**, 217003 (2001).

[9] M. Zgirski, K.-P. Riikonen, V. Touboltsev, and K. Yu. Arutyunov, Phys. Rev. B **77**, 054508 (2008).

[10] G. Schön and A. D. Zaikin, Phys. Rep. **198**, 237 (1990).

[11] A. van Otterlo, D. S. Golubev, A. D. Zaikin, and G. Blatter, Eur. Phys. J. B **10**, 131 (1999).
[12] S. V. Panyukov and A. D. Zaikin, J. Low Temp. Phys. **73**, 1 (1988).
[13] D. V. Averin and A. A. Odintsov, Phys. Lett. A **140**, 251 (1989).
[14] A. D. Zaikin, J. Low Temp. Phys. **80**, 223 (1990).
[15] J. E. Mooij and Yu. V. Nazarov, Nat. Phys. **2**, 169 (2006).
[16] A. G. Semenov, Ph.D. thesis, P. N. Lebedev Physics Institute, Russia, 2010.
[17] A. M. Hriscu and Yu. V. Nazarov, Phys. Rev. B **83**, 174511 (2011).
[18] A. G. Semenov and A. D. Zaikin, Phys. Rev. B **88**, 054505 (2013).
[19] J. E. Mooij and G. Schön, Phys. Rev. Lett. **55**, 114 (1985).
[20] For the sake of simplicity, here we assume that $v\tau_0 \sim x_0$, where $x_0 \sim \xi$ is the QPS core size in space.
[21] D. S. Golubev and A. D. Zaikin, Phys. Rev. B **78**, 144502 (2008).
[22] Experimental evidence for quantum coherent behavior of QPSs was demonstrated by O. V. Astafiev *et al.*, Nature (London) **484**, 355 (2012).
[23] Due to momentum conservation, plasmons can only be created in pairs with the total zero momentum.
[24] See, e.g., D. Controzzi, F. H. L. Essler, and A. M. Tsvelik, Phys. Rev. Lett. **86**, 680 (2001), and references therein.
[25] J. E. Mooij and C. J. P. M. Harmans, New J. Phys. **7**, 219 (2005).